Pol. J. Environ. Stud. Vol. 31, No. 4 (2022), 3455-3462
DOI: *10.15244/pjoes/145412* ONLINE PUBLICATION DATE: 2022-04-07

Original Research

Soil-Water Characteristic Curves and Fitting Models of Collapsible Loess: A Case Study of Lanzhou, China

Wenju Zhao[1]*, Chun Zhou[1], Jiazhen Hu[1], Fangfang Ma[1], Zhijun Wang[1,2]

[1]College of Energy and Power Engineering, Lanzhou University of Technology, Lanzhou 730050, China
[2]Baiyin New Material Research Institute of Lanzhou University of Technology, Baiyin 730900, China

Received: 10 October 2021
Accepted: 29 December 2021

Abstract

The soil-water characteristic curve (SWCC) is an important hydrodynamic representation of soil and the basis for studying the water content of collapsible loess. The objectives of this study were to determine the water holding capacity of collapsible loess and the best fitting model of SWCC. We selected representative samples of collapsible loess in Lanzhou and measured the SWCCs. The SWCCs for soil samples varied with bulk density and particle size. The shapes were the same, but the volumetric water content (VWC) decreased as the suction increased. The suction of different soil layers tended to first decrease rapidly, then decrease more gradually and finally stabilize with VWC. The fitted VWC for the VG model was closer to the measured content, and the accuracy of the model was high. The VG-M (1-1/*n*, *n*) model was the best of the six models tested and was selected as the optimal model for fitting SWCCs, which will provide a theoretical basis for the accurate fitting of data of collapsible loess.

Keywords: soil moisture characteristic curve, VG model, BC model, collapsible loess in Lanzhou

Introduction

The soil-water characteristic curve (SWCC) is a hydrodynamic representation of soil for studying the effects of the expansion or contraction of soil on texture, structure, bulk density, temperature and pores and is the basis of studying soil hydrodynamics [1-2]. The soil porosity of different particle sizes is different. The smaller the soil particle size is, the denser its pore structure is, the medium and small voids increase and the connectivity becomes poor. The water holding capacity of unsaturated remolded loess decreases with the increase of temperature, and the temperature effect decreases with the increase of temperature or the decrease of water content. The change of water characteristic curve of coarse sand is the steepest, and the change of water characteristic curve of tight sand, light loam, medium loam and heavy loam is gentle [3-5]. SWCC models and factors influencing SWCCs have been well studied [6-8]. Xing [9] found that the van Genuchten model was optimal for fitting the SWCCs of four types of soil. Phoon [10] demonstrated that a lognormal random vector is suitable to model the curve-fitting parameters of the SWCC. Liu [11] reported that the Gardner model was better than the models

*e-mail: wenjuzhao@126.com

of van Genuchten, Fredlund and Xing for an area erosion of collapsible soil near the city of Ganzhou. Zhao [12] believed that the fitting accuracy for sand-mulched land was higher for the van Genuchten than the Brooks Corey model. Kong [13] used the modified van Genuchten model in terms of cumulative pore volume to obtain the best-fit POSD of the drying-wetting cycle samples.

SWCCs have been constructed for various soils. Fattah [14] found that SWCCs differed among bulk densities and that an increase in bentonite content had little effect on the SWCCs. Zhou [15] proposed that changes of soil physical composition, particle size and dry density would affect SWCCs, and Fattah [16] Compared the effects of soil saturation method and soil saturation method on SWCC and showed that the capillary rise saturation gives a higher value than the top surface water top and the variable water content method for both wetting and drying SWCC cases. Khlosi [17] found that the plastic limit, texture, carbonate content, specific surface area and bulk density of 11 chemical and physical soil properties affected SWCCs. Zhao [18] presented a case study of the temporal stability and variability of SWC at various depths which shows that the monitoring of field-mean SWC over a long period of time from representative locations is feasible.

Collapsible loess is a typical wind-formed deposit widely distributed in arid and semi-arid areas of Northwest China [19]. Soil structure will be rapidly destroyed, and soil will subside under sufficient pressure, rapidly reducing soil strength [20-21]. The collapsible deformation of loess subgrade when water-logged could lead to unacceptable deformations in loess areas [22]. Pore distribution and the micro rule of the collapsible loess in Lanzhou, however, have rarely been analyzed using SWCCs. The objectives of this study are to construct SWCCs of soils of different bulk densities, particle sizes and depths of collapsible loess, study the variation of the suction and volumetric water content (VWC) of collapsible loess in the Lanzhou area, determine the optimal model suitable for the soil water characteristic curve of collapsible loess. Our results provide a theoretical basis for managing soil water and soil collapse erosion improvement design of collapsible loess.

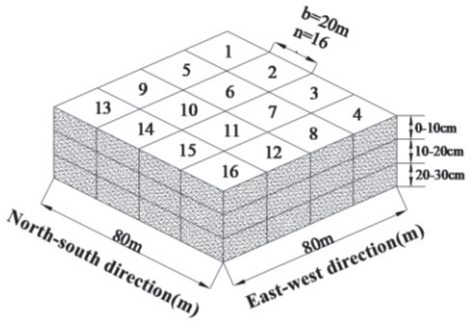

Fig. 2. distribution of sampling points.

Materials and Methods

Soil Sampling

The study area of collapsible loess is Peng Jia Ping Town, Lanzhou, Gansu Province, China (103°44'N, 36°03'E) (Fig. 1) in the Yellow River Basin. The soil is a silty clayey loam, which is a typical collapsible loess. The study area was 22.8 km^2, and we selected 80m×80m as a representative plot. The samples were collected from July to November 2019 and from July to November 2020. A mechanical sampling scheme was adopted, and the 0-30 cm layer at the center of the plot was excavated every 20 m along the east-west and north-south directions, with 16 sampling points in each of the 0-10, 10-20 and 20-30 cm layers (Fig. 2). A ring knife was used to measure bulk density at each sampling point, which ranged from 1.38 to 1.58 g/cm^3. We used bulk densities of 1.38, 1.48 and 1.58 g/cm^3 to facilitate centralized management for manual filling.

Research Methods

(1) van Genuchten (VG) model:

$$\theta(\mathrm{h})=\begin{cases}\theta_r+\dfrac{\theta_s-\theta_r}{\left(1+|\alpha h|^n\right)^m} & h<0\\ \theta_s & h\geq 0\end{cases} \quad (1)$$

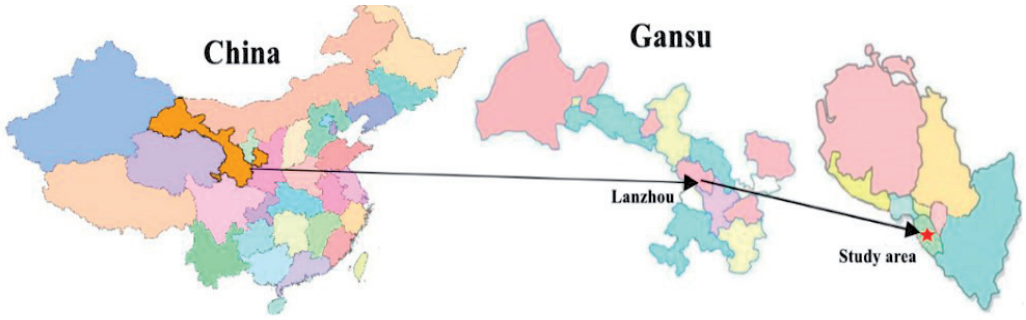

Fig. 1. Geographical location of the study area.

where h is the soil suction, cm; α is the reciprocal of the air inlet value, cm^{-1}; θ is the VWC, cm^3/cm^3; θ_s is the saturated VWC, cm^3/cm^3; θ_r is the residual VWC, cm^3/cm^3, and m and n are shape coefficients. n determines the slope of an SWCC: the curve is steeper when n is larger [23]. Van Genuchten model is widely used because of its high fitting accuracy and clear physical meaning of parameters [24].

(2) Saturation form of the van Genuchten (VG-M) model:

$$s = \frac{1}{\left[1+(\alpha h)^n\right]^m} \quad (2)$$

where s is saturation. The VG model is developed into the Mualem model when m = 1-1/n, which is commonly used in geotechnical engineering [25].

(3) Brooks Corey (BC) model:

$$\frac{\theta - \theta_r}{\theta_s - \theta_r} = \begin{cases} (\alpha h)^{-n} & \alpha h > 1 \\ 1 & \alpha h < 1 \end{cases} \quad (3)$$

Brooks Corey model is simple in form and has been widely used. The model simulates the soil water movement with coarse structure, and the results are satisfactory [26].

The accuracy of the appeal model is verified by the sum of squares (SSQ) and the coefficient of determination (R^2).

Results and Discussion

Effects of Bulk Density and Particle Size on SWCCs

Differences among the SWCCs under different bulk densities and particle sizes were determined using an indoor centrifugal experiment (Fig. 3). The experimental process of this paper is to evenly load the air dried soil samples into the ring knife according to the preset bulk density, soak them in distilled water for 48 hours, and then determine the soil moisture characteristic curve in the high-speed constant temperature freezing centrifuge. The constant temperature in the centrifuge is 4ºC, and the suction range is set to 10-7000 cm.

SWCCs (Fig. 3a) were constructed for the soil samples with different bulk densities (1.38, 1.48, and 1.58 g/cm^3) and a particle size of 2 mm at the same volume. The higher the bulk density, the lower the initial VWC. VWC decreased as the bulk density increased under the same suction, and the total volume of soil pores also changed, indicating that the denser the soil, the higher the bulk density, the smaller pores and the more difficult the pore water to drain.

We analyzed the SWCCs for different particle sizes (1 and 2 mm) under the same dry bulk density

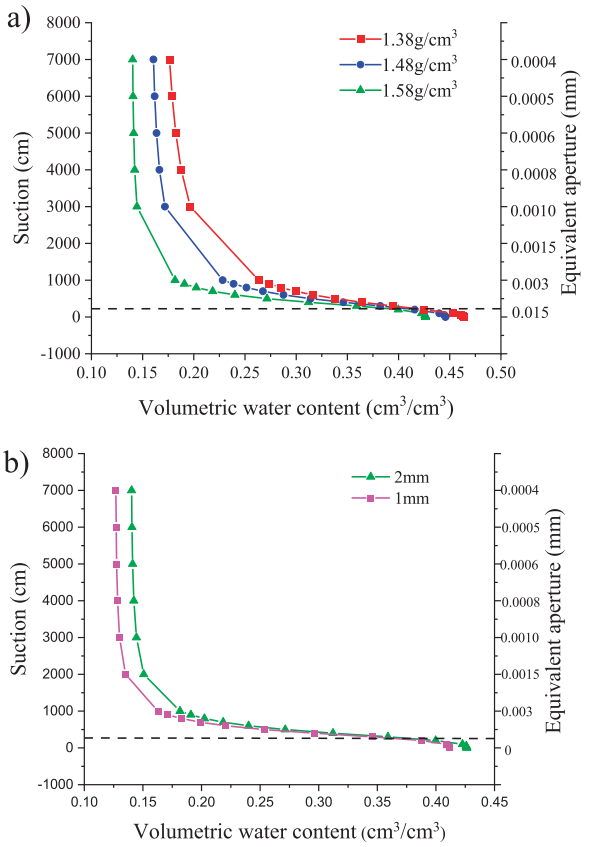

Fig. 3. Soil-water characteristic curve of different bulk density and particle size. a) different bulk density, b) different particle size.

(1.58 g/cm^3) (Fig. 3b) to determine the effect of particle size on the water-holding capacity of the soil. VWC was higher for the 1-mm than the 2-mm particles at the same suction, and the suction was higher for the 2-mm than the 1-mm particles under the same VWC. The SWCCs for the different particle sizes almost overlapped in the low-suction section, and the rate of water discharge was higher, but the trend of change in VWC was slower as suction increased.

Effect of Soil Depth on SWCCs

Soil suction for the soil layers tended to first decrease rapidly, then decrease more gradually and finally stabilize with VWC (Fig. 4). The decrease in VWC was largest at low levels of suction (<1000 cm), the SWCCs changed steadily and the specific water capacity was larger. As suction increased, the curves became steeper, pore drainage decreased and the specific water capacity decreased. Soil drainage mainly comes from the change of water in capillary pores at intermediate levels of suction (1000-7000 cm). The range of water change was small and the SWCCs were steep due to the strong capacity of the soil to absorb water. VWC increased with depth at the same level of suction (Fig. 4).

The amount of water retained or released by the soil mainly depends on the larger pores of the soil structure.

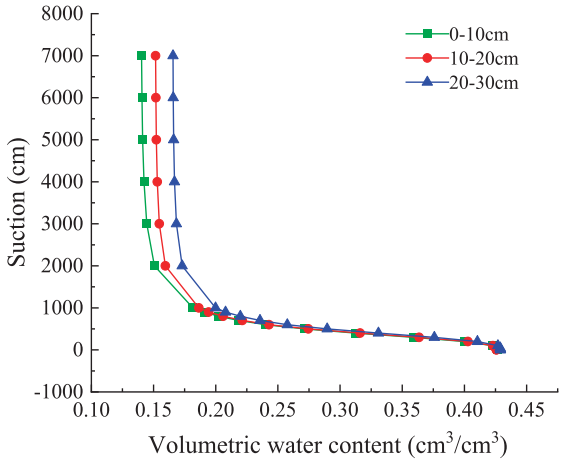

Fig. 4. Soil-water characteristic curve at different depths.

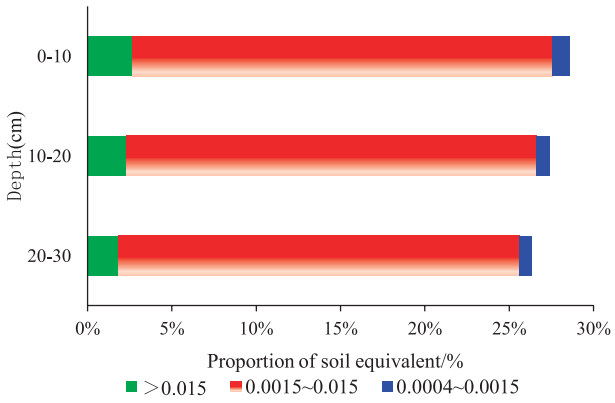

Fig. 5. Distribution proportion of equivalent pore size of soil at different depths.

When the equivalent pore diameter of soil is within the range of 0.0015~0.015 mm (Fig. 5), the proportion of equivalent pore diameter of soil is the largest, and the proportion of equivalent pore diameter of 0~10 cm, 10~20 cm and 20~30 cm of each layer of soil is 24.91%, 24.34% and 23.75% respectively. In general, with the increase of soil depth, the proportion of soil equivalent pore size decreases, and the stronger the soil water holding capacity, the size of soil equivalent pore size is negatively correlated with soil water holding capacity.

Determination of the Optimal SWCC Model

The VG and BC models, which are widely used, were selected and combined with the Mualem and Burdine models of hydraulic conductivity of unsaturated soil, and the relationship between m

Table 1. Fitting values and fitting errors of hydraulic parameters of different soil bulk density models.

Layer cm	Soil type	Fitting model	θ_r cm³/cm³	θ_s cm³/cm³	α cm⁻¹	m	n	R^2	SSQ
0~10	1.58g/cm³	VG-M(m, n)	0.1394	0.4263	0.0026	0.6741	2.9080	0.9979	0.0006
		VG-M(1-1/n, n)	0.1393	0.4263	0.0026		2.9365	0.9999	0.0000
		BC-M	0	0.4255	0.0066		0.3663	0.9699	0.0080
		VG-B(m, n)	0.1394	0.4263	0.0026	0.6741	2.9080	0.9979	0.0006
		VG-B(1-2/n, n)	0	0.4328	0.0066		2.3710	0.9629	0.0099
		BC-B	0	0.4255	0.0067		0.3663	0.9670	0.0080
0~10	1.48g/cm³	VG-M(m, n)	0.1558	0.4459	0.0025	0.5956	2.3937	0.9985	0.0004
		VG-M(1-1/n, n)	0.1556	0.4459	0.0026		2.4111	0.9999	0.0000
		BC-M	0	0.4444	0.0064		0.3127	0.9865	0.0300
		VG-B(m, n)	0.1558	0.4459	0.0025	0.5956	2.3937	0.9985	0.0004
		VG-B(1-2/n, n)	0	0.4504	0.0061		2.3230	0.9820	0.0044
		BC-B	0	0.4444	0.0064		0.3127	0.9865	0.0300
0~10	1.38g/cm³	VG-M(m, n)	0.1613	0.4636	0.0027	0.5118	1.9922	0.9991	0.0002
		VG-M(1-1/n, n)	0.1609	0.4635	0.0028		2.0074	0.9997	0.0003
		BC-M	0	0.4607	0.0065		0.2755	0.9945	0.0013
		VG-B(m, n)	0.1611	0.4635	0.0027	0.5055	2.0050	0.9991	0.0002
		VG-B(1-2/n, n)	0	0.4658	0.0061		2.2876	0.9929	0.0016
		BC-B	0	0.4607	0.0065		0.2755	0.9945	0.0013

Note: When the fitted value of θ_r is less than 0.001, the RETC software automatically selects its value as 0.

and n in the VG model were fully considered. We therefore used six models, VG-M (*m*, *n*), VG-M (1-1/*n*, *n*), BC-M, VG-B (*m*, *n*), VG-B (1-2/*n*, *n*) and BC-B, to fit and analyze the experimental data of the SWCCs for different bulk densities (Table 1) and soil depths (Table 2). The error between the measured and fitted VWCs under different levels of suction was analyzed, and the fitting accuracies of the models were characterized using the sum of squares (*SSQ*) and the coefficient of determination (R^2) for identifying the optimal fitting model for Lanzhou collapsible loess.

Each fitting model was applicable to soil under different bulk densities, with R^2 >0.9629, small relative errors and high fitting accuracies (Table 1). The measured and fitted values were more similar for the VG than the BC model, and the accuracy was high.

The fitting accuracy of each model for soil at different depths was high: R^2 was >0.9491, the relative error was small and the fitting accuracy was high (Table 2). The VG model combined with the models of unsaturated hydraulic conductivity (Mualem and Burdine models), Mualem model had a higher fitting accuracy. The BC model and the models of unsaturated hydraulic conductivity did not differ significantly. We therefore selected the VG-M (1-1/*n*, *n*) model, which had the highest correlation coefficient, the lowest *SSQ*, the highest R^2 and the best simulation, as the optimal model for the collapsible loess in Lanzhou.

The measured data for the various factors were fitted using RETC software. The VG-M (1-1/*n*, *n*) model was selected. The SWCCs were constructed with soil suction as the x-axis and VWC as the y-axis (Fig. 6). The red points in the figure are the measured values, and the black solid line is the fitted VG-M (1-1/*n*, *n*) curve. Most of the measured VWCs of the Lanzhou collapsible loess under the various factors were on the fitted curve, further indicating that the VG-M (1-1/*n*, *n*) model had high fitting accuracy and was the optimal model for the Lanzhou collapsible loess.

Discussion

Collapsible loess is affected by rainfall, soil porosity, the soil matrix and other factors, so SWCCs vary greatly in space and with scale. Bordoni [27] reported that the distribution of pore size could be indirectly represented by SWCCs and that pore size directly affected the movement of water and solutes in soil. Li [28] found that lime-treated collapsible loess became saturated more than untreated loess under the same matric suction. The collapsible loess is widely

Table 2. Fitting values and fitting errors of hydraulic parameters for different soil depths.

Layer cm	Soil type	Fitting model	θ_r cm^3/cm^3	θ_s cm^3/cm^3	α cm^{-1}	*m*	*n*	R^2	*SSQ*
0~10	1.58g/cm^3	VG-M(*m*, *n*)	0.1265	0.4118	0.0026	0.6996	3.0580	0.9978	0.0006
		VG-M(1-1/*n*, *n*)	0.1263	0.4117	0.0026		3.0820	0.9990	0.0011
		BC-M	0	0.4112	0.0065		0.4016	0.9668	0.0090
		VG-B(*m*, *n*)	0.1265	0.4118	0.0026	0.6996	3.0580	0.9812	0.0051
		VG-B(1-2/*n*, *n*)	0	0.4186	0.0064		2.4066	0.9590	0.0110
		BC-B	0	0.4112	0.0065		0.4016	0.9668	0.0090
10~20	1.58g/cm^3	VG-M(*m*, *n*)	0.1512	0.4257	0.0026	0.7001	3.0715	0.9979	0.0006
		VG-M(1-1/*n*, *n*)	0.1510	0.4256	0.0026		3.1141	0.9998	0.0002
		BC-M	0	0.4300	0.0311		0.1702	0.9610	0.0359
		VG-B(*m*, *n*)	0.1512	0.4257	0.0026	0.7001	3.0715	0.9865	0.0300
		VG-B(1-2/*n*, *n*)	0	0.4326	0.0070		2.3424	0.9534	0.0116
		BC-B	0	0.4251	0.0069		0.3341	0.9610	0.0097
20~30	1.58g/cm^3	VG-M(*m*, *n*)	0.1652	0.4290	0.0025	0.7034	3.1657	0.9995	0.0005
		VG-M(1-1/*n*, *n*)	0.1654	0.4289	0.0025		3.1983	0.9997	0.0003
		BC-M	0	0.4285	0.0068		0.3136	0.9571	0.0100
		VG-B(*m*, *n*)	0.1652	0.4290	0.0025	0.7034	3.1657	0.9978	0.0005
		VG-B(1-2/*n*, *n*)	0	0.4359	0.0070		2.3141	0.9491	0.0118
		BC-B	0	0.4285	0.0068		0.3136	0.9571	0.0100

Note: When the fitted value of θ_r is less than 0.001, the RETC software automatically selects its value as 0.

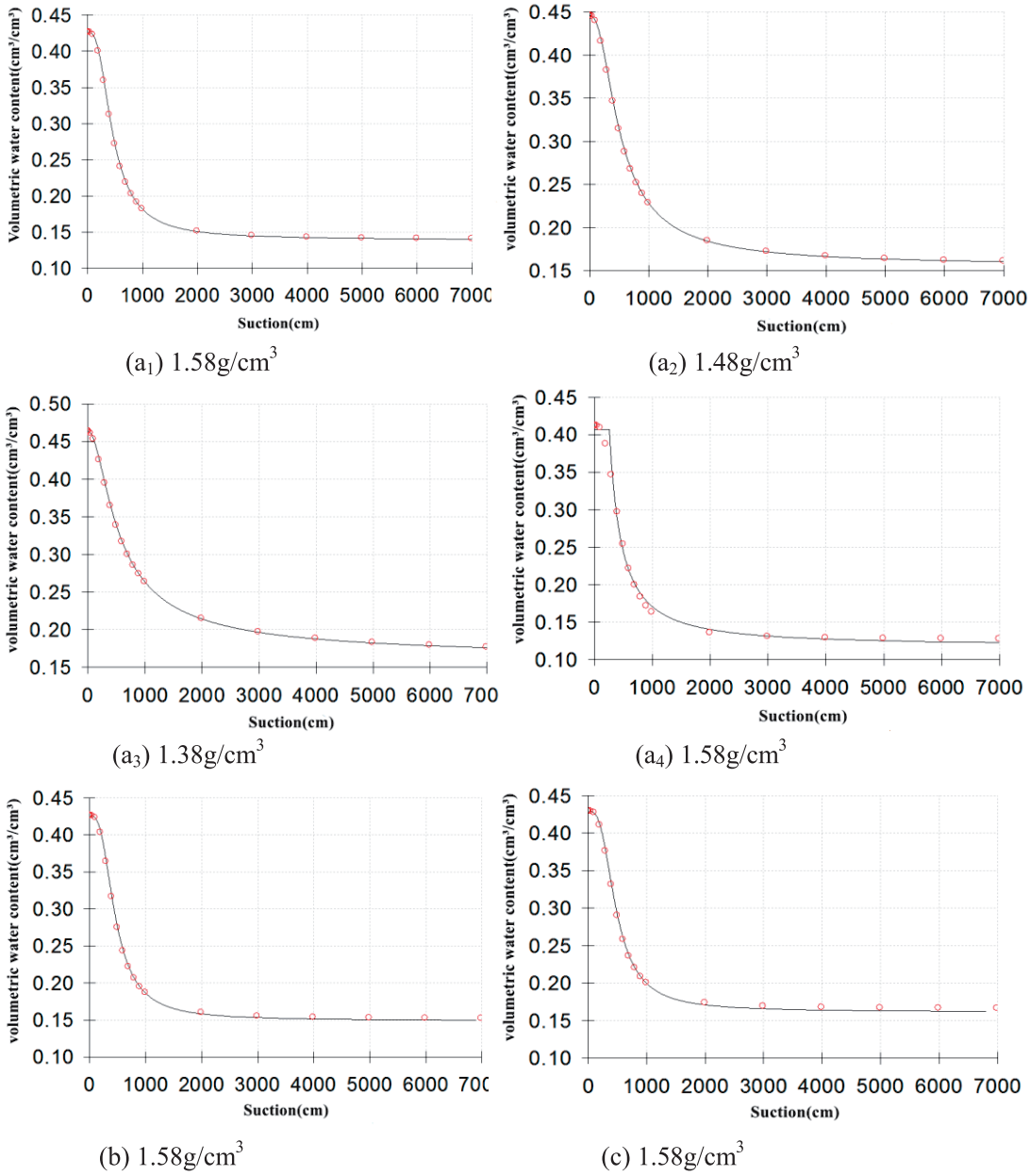

Fig. 6. Fitting curve of soil moisture characteristic curve.
Note: (a_1), (a_2), (a_3), (a_4) are 0-10 cm soil layer, b is 10-20 cm soil layer, c is 20-30 cm soil layer.

distributed in Lanzhou. Therefore, we studied the pore distribution of collapsible loess soil under different bulk density, particle size and depth. The results show that the larger the soil bulk density is, the smaller the pore is, and the stronger the soil water holding capacity is. Under the same soil water suction condition, with the deepening of the soil layer, the soil volume moisture content increases, revealing the influence of different factors on the soil water holding capacity. It is expected to provide guidance for soil water management in collapsible loess area.

Many studies have identified optimal SWCC fitting models suitable for different regions and soil types. Rojas [29] proposed a porous solid model to simulate the influence of soil-water lag and volume deformation on SWCCs. Some studies used the VG and Gardner models to fit and analyze SWCCs for different soil types. [30] The VG model fitted the data the best and had a high fitting accuracy. The optimal VG model suitable for different planting years in sand pressing field was determined by Zhao [31]. Our study analyzed SWCCs for different bulk densities, particle sizes and depths using six models. The VG-M (1-1/n, n) model had the highest fitting accuracy and was more suitable for constructing SWCCs for the collapsible loess in Lanzhou. Our results provide an important basis for further study of the collapse and erosion of collapsible soil and the design of soil cover in Lanzhou, especially when considering other factors such as texture and vegetation. Water properties of various types of soil

(MWD, AWC, K, POR, PAW) and the dependence of the SWCC curve shape on the water properties of various soils, further research will be done in the future.

Conclusions

This paper used SWCCs for collapsible loess in typical area of Lanzhou under different bulk densities, particle sizes and depths to analyze soil suction and VWC and to identify the best fitting model.

1. The SWCCs were consistent for the different bulk densities and particle sizes. Bulk density decreased and particle size increased as VWC increased under the same soil suction. Soil suction in different soil layers tended to first decrease rapidly, then decrease more gradually and finally stabilize with VWC. The proportion of pores of equal size decreased, and the water-holding capacity of the soil increased, with soil depth. In practical engineering application, it can increase the drainage measures of deep soil to prevent loess from collapsing.
2. The measured and fitted values were more similar for the VG than the BC model, and the accuracy was higher. The Mualem model was the best for simulating unsaturated hydraulic conductivity under various factors. The VG-M (1-1/*n*, *n*) model, with the best simulation, was therefore selected for fitting the SWCCs for Lanzhou collapsible loess. It can provide a theoretical basis for the construction and treatment of collapsible loess project in Lanzhou.

Acknowledgments

This study was supported by the National Natural Science Foundation of China (51869010), Ministry of Agriculture Open Fund Project (2017001), Guidance Program for Industrial Support of Colleges and Universities in Gansu Province (2019C-13), Demonstration of key technologies for green development of industrialized ecological agriculture in Jingtai desert Gobi (20YF8ND141).

Conflict of Interest

The authors declare no conflict of interest.

References

1. MESKINI V.F., MOHAMMADI M.H., VANCLOOSTER M. Predicting the soil moisture retention curve, from soil particle size distribution and bulk density data using a packing density scaling factor. Hydrology and Earth System Sciences, **18** (10), 4053, **2014**.
2. ZHAO W.J., CUI Z., ZHANG J.Y., JIN J. Temporal stability and variability of soil-water content in a gravel-mulched field in northwestern China. Journal of Hydrology, **552**, 249, **2017**.
3. CUI Z.Z., ZHOU W.H., PAN P., LI J.. Thixotropic characteristics of remolded loessin Tongxin County Ningxia.Hydroelect. Engineer. **35** (6), 111, **2016**.
4. WANG W.M., GUO S.C., CUI Z.Z. Study of effect of soluble salt on loess thixotropy. Rock and Soil Mechanics **35** (12), 3386, **2014**.
5. YAN Y.J., WEN B.P., HUANG Z.Q. Effect of soluble salts on shear strength of unsaturated remoulded loess in Lanzhou city. Rock and Soil Mechanics **38** (10), 2881, **2017**.
6. VAN G.M.T. A closed-form equation for predicting the hydraulic conductivity of unsaturated soils. Soil Science Society of America Journal, **44** (5), 892, **1980**.
7. ZIMMERMAN R.W., BODVARSSON G.S. A simple approximate solution for horizontal infiltration in a Brooks-Corey medium. Transport in Porous Media, **6** (2), 195, **1991**.
8. FREDLUND D.G., XING A. Equations for the soil-water characteristic curve. Canadian Geotechnical Journal, **31** (4), 521, **1994**.
9. XING X., ZHAO W., MA X., ZHANG Y. Study on soil shrinkage characteristics during determination of soil moisture characteristic curve. Journal of water conservancy, **46** (10), 1181, **2015**.
10. PHOON K.K., SANTOSO R., QUEK. T. Probabilistic analysis of soil-water characteristic curves. Journal of Geotechnical & Geoenvironmental Engineering, **136** (3), **2010**.
11. LIU W.P., LUO X.Y., FU M.F., HUANG J.S. Experiment and Modeling of Soil-Water Characteristic Curve of Unsaturated Soil in Collapsing Erosion Area. Polish Journal of Environmental Studies, **25** (6), 2509, **2016**.
12. ZHAO W.J., CAO T.H., LI Z.L., SU Y., BAO Z.Y. Spatial variability of the parameters of soil-water characteristic curves in gravel-mulched fields. Water Science and Technology-Water Supply, **20** (1), 231, **2020**.
13. KONG L., SAYEM H.M., TIAN H. Influence of drying-wetting cycles on soil-water characteristic curve of undisturbed granite residual soils and microstructure mechanism by nuclear magnetic resonance (nmr) spin-spin relaxation time (t2) relaxometry. Canadian Geotechnical Journal, cgj-2016-0614, **2017**.
14. FATTAH M.Y., SALIM N.M., IRSHAYYID E.J. Determination of the soil-water characteristic curve of unsaturated bentonite-sand mixtures. Environmental Earth Sciences,**76** (5), 201, 1-12, **2017**.
15. ZHOU W.G., BAO Y.L., ZHOU H.B. Research on Soil-Water Characteristic Curve of Unsaturated Mixed-Soil in West Sichuan. Applied Mechanics and Materials, **353-356**, 996, **2013**.
16. FATTAH M.Y., MAJEED Q.G., JONI H.H. Comparison between methods of soil saturation on determination of the soil water characteristic curve of cohesive soils. Arabian Journal of Geosciences, **14** (2), **2021**.
17. KHLOSI M., CORNELIS W.M., DOUAIK A., HAZZOURI A., HABIB H., GABRIELS D. Exploration of the Interaction between Hydraulic and Physicochemical Properties of Syrian Soils. Vadose Zone Journal, **12** (4), **2013**.
18. ZHAO W.J., CUI Z., ZHOU C. Spatiotemporal variability of soil-water content at different depths in fields mulched with gravel for different planting years. Journal of Hydrology, **590**, 125253, **2020**.
19. HAERI S. MOHSEN, GARAKANI, AMIR A., ROOHPARVAR, HAMID R., DESAI, CHANDRAKANT S., GHAFOURI S. MOHAMMAD

H.S., KOUCHESFAHANI KASRA S. Testing and constitutive modeling of lime-stabilized collapsible loess. I: experimental investigations. International Journal of Geomechanics, **19** (4), 04019006, **2019**.
20. ZHANG Y.J., LI J.D., WANG X., LI F., LI S., MA X.N. Experimental study on water immersion of diaphragm wall on collapsible loess foundation. Journal of geotechnical engineering, **40** (1), 73, **2018**.
21. GUAN W.W. New chapter on engineering performance of collapsible loess. Xi'an Jiaotong University, Xi'an. **1992**.
22. REN W., YANG T., HUANG M., ZHANG A., HU J. Optimal mixing ratio and SWCC fitting of lightweight soil with cotton stalk fibres. Soils and Foundations Tokyo, **61** (1), **2021**.
23. LI P., LI T.L., VANAPALLI S.K. Prediction of soil-water characteristic curve for Malan loess in Loess Plateau of China. Journal of Central South University, **25** (2), 432, **2018**.
24. HUANG S.Y., BARBOUR S.L., FREDLUND D.G. Development and verification of a coefficient of permeability function for a deformable unsaturated soil. Canadian Geotechnical Journal **35** (3), 411, **1998**.
25. LEI Z.D., YANG S.X., XIE S.Z. Soil hydrodynamics. Tsinghua University, Beijing, **1988**.
26. GALLIPOLI D., WHEELER S., KARSTUNEN M. Modelling the variation of degree of saturation in a deformable unsaturated soil. Geotechnique, **53** (1), 105, **2003**.
27. BORDONI M., BITTELLI M., VALENTINO R., et al. Improving the estimation of complete field soil water characteristic curves through field monitoring data [J]. Journal of Hydrology, **2017**, 552:283-305. DOI: 10.1016/j.jhydrol.2017.07.004
28. LI X., HU C., LI F., et al. Determining soil water characteristic curve of lime treated loess using multiscale structure fractal characteristic [J]. Scientific Reports, **10** (1), **2020**, DOI: 10.1038/s41598-020-78489-7
29. ROJAS E., CHAVEZ O., ARROYO H. Modeling the Dependency of Soil-Water Retention Curve on Volumetric Deformation. International Journal of Geomechanics, **17** (1), 1, **2017**.
30. ETMINAN S., JALALI V., MAHMOODABADI M. Assessing an efficient hybrid of Monte Carlo technique (GSA-GLUE) in Uncertainty and Sensitivity Analysis of van Genuchten Soil Moisture Characteristics Curve. Computational Geosciences, **25**, 503, **2021**.
31. ZHAO W.J., CAO T.H., LI Z.L. Spatial variability of the parameters of soil-water characteristic curves in gravel-mulched fields. Water Science and Technology-Water Supply, **20** (1), 231, **2020**.